THE JOURNAL OF PHYSICAL CHEMISTRY C

Article

pubs.acs.org/JPCC

Investigating the Energetic Ordering of Stable and Metastable TiO_2 Polymorphs Using DFT+*U* and Hybrid Functionals

Matthew T. Curnan[†] and John R. Kitchin*[,‡]

[†]Department of Materials Science and Engineering and [‡]Department of Chemical Engineering, Carnegie Mellon University, 5000 Forbes Ave., Pittsburgh, Pennsylvania 15213, United States

Supporting Information

ABSTRACT: Prediction of transition metal oxide BO_2 (B = Ti, V, etc.) polymorph energetic properties is critical to tunable material design and identifying thermodynamically accessible structures. Determining procedures capable of synthesizing particular polymorphs minimally requires prior knowledge of their relative energetic favorability. Information concerning TiO_2 polymorph relative energetic favorability has been ascertained from experimental research. In this study, the consistency of first-principles predictions and experimental results involving the relative energetic ordering of stable (rutile), metastable (anatase and brookite), and unstable (columbite) TiO_2 polymorphs is assessed via density functional theory (DFT). Considering the issues involving electron−electron interaction and charge delocalization in TiO_2 calculations, relative energetic ordering predictions are evaluated over trends varying Ti Hubbard U_{3d} or exact exchange fraction parameter values. Energetic trends formed from varying U_{3d} predict experimentally consistent energetic ordering over U_{3d} intervals when using GGA-based functionals, regardless of pseudopotential selection. Given pertinent linear response calculated Hubbard *U* values, these results enable TiO_2 polymorph energetic ordering prediction. Hybrid functional calculations involving rutile−anatase relative energetics, though demonstrating experimentally consistent energetic ordering over exact exchange fraction ranges, are not accompanied by predicted fractions, for a first-principles methodology capable of calculating exact exchange fractions precisely predicting TiO_2 polymorph energetic ordering is not available.

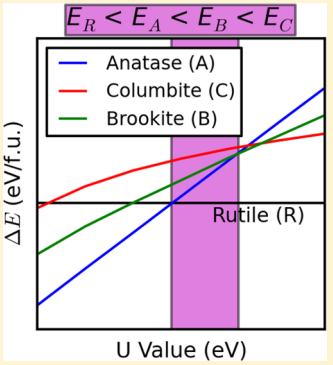

INTRODUCTION

Transition metal dioxides characterized as BO_2 are used in applications that involve supportive substrates in CO oxidation processes,[1−3] photocatalysis,[4,5] electrochemical water splitting,[6,7] electrode coating and doping,[8−10] gas sensing for controlling engine fuel consumption,[11,12] cleaning automative exhaust,[13,14] and electronic devices.[3,15] In several of the applications that are listed above and others,[16−18] the accurate characterization of properties, such as band gap[19,20] and the temperature and pressure dependence of phase stability,[21,22] of oxide materials is critical.

With respect to most photochemical applications, anatase is the most photocatalytically active TiO_2 polymorph that naturally forms under ambient conditions,[5,11,23] though its wide band gap (E_g = 3.0−3.2 eV) limits its solar energy conversion efficiency.[19,24,25] Recent theoretical studies have postulated that the TiO_2 band gap can be tuned by changing its polymorphic structure from that of anatase (tetragonal) to a cubic structure such as fluorite[19,20] or pyrite.[26,27] The thermodynamic stability of these cubic phases under particular reaction conditions has been considered experimentally[28−30] and theoretically,[31−33] though none of these studies conclusively characterize their stability.

Despite the enhanced recombination effects potentially resulting from doping,[26] mixed-metal oxides composed of fluorite-structured CeO_2 and anatase-structured TiO_2 have also been employed to tune the band gap, additionally improving catalyst properties such as effective surface area and thermostability.[1,2,13,24] Varying CeO_2 composition can tune the band gap to maximize visible light absorption in TiO_2−CeO_2 catalysts[34] and substantially improve their photochemical activity without known negative consequences.[35] With particular consideration to phase stability, materials property characterization can only be fully addressed via a comprehensive methodology applicable to a broad materials set. Applications such as CO oxidation employing BO_2 supports[3] and epitaxial stabilization[36,37] employ metal oxide candidates featuring a wide range of transition metal cations (B = Ti, V, Cr, Mn, Ru, Ir).[3,37]

Density functional theory (DFT) has been previous applied as a computationally efficient[38,39] component of a methodology capable of predictively characterizing broad sets of metal oxide properties ranging from relative energetic stability[40−42] to electronic structure.[43,44] Furthermore, this methodology should also be able to minimally predict the relative ordering of values of properties,[42] such as the formation energy ordering of various TiO_2 polymorphs,[37,45] that are close in value consistently.[37,42,45] However, previous use of DFT to determine the relative energetics of TiO_2[37,45,46] structures has yielded functional-dependent results. Across the development of

Received: June 4, 2015
Revised: August 7, 2015
Published: August 12, 2015

DOI: 10.1021/acs.jpcc.5b05338
J. Phys. Chem. C 2015, 119, 21060−21071

different basis sets and orbital overlap criteria, use of the LDA functional consistently predicts the relative energetic favorability of rutile relative to anatase, serving as the only functional capable of consistently demonstrating bulk rutile to be more energetically favorable than bulk anatase over multiple basis sets and orbital overlap criteria. Under a single basis set and orbital overlap criteria combination, the use of pure HF exchange can also achieve the relative energetic favorability of rutile, while all other combinations of input produce HF functional results with lower relative energetic differences favoring anatase than the corresponding energetic differences produced by non-LDA functionals. In all other tested combinations of basis set and orbital overlap criteria, spanning consideration of HF, LDA, PBE, PBE0, and B3LYP functionals, anatase is predicted to be more energetically favorable than rutile.[46]

Experimentally and theoretically, the relative phase stability of TiO_2 polymorphic structures has been determined to be strongly affected by particle size,[8,12,47] particle shape,[26,48] pressure and temperature conditions during synthesis,[47,49,50] and the solvent surrounding that phase.[47,48] Studies completed using the ReaxFF method[51] have begun to characterize the relationships between phase stability and these factors[52,53] instead of DFT due to computational cost.[54,55] Surface structural configurations,[56] atomic bond lengths and angles,[53,55] and bulk structure equations of state (EOS)[52,54] calculated with DFT are used to parametrize ReaxFF calculations; thus, accurate electronic structure calculations are still needed to reliably characterize TiO_2 phase stability.

Though the reasons for the inconsistent energetic ordering results for TiO_2 across functionals are still contested,[57] a probable source is the nonsystematic error incurred by unphysical electron−electron interactions,[58,59] which is commonly observed in 3d transition metal oxide DFT calculations completed using standard local density (LDA) and generalized gradient (GGA) approximation functionals.[40,60] The electron−electron interaction error in these calculations can be accounted for using hybrid functionals such as PBE0 and HSE06, in which the delocalization of 3d Ti electron charge density typical in standard functionals is countered by the matching localization effects induced by employing exact Hartree−Fock (HF) exchange.[61]

Considering that the relative energetic ordering of rutile and anatase TiO_2 polymorphs can change when switching between using standard functionals[25,32] and exact HF exchange,[62] hybrid functionals can apparently resolve the correct relative energetics of TiO_2 polymorphs albeit with large computational expense.[38] Though physical electron delocalization behavior was achieved using 20% HF exchange with Lee, Yang, and Parr correlation in these TiO_2 polymorphs,[63] physically reasonable behavior was not achieved in oxides such as NiO using this amount of HF exchange.[63,64] Thus, the use of a single percentage of HF exchange cannot be generalized over many materials and cannot be applied to a predictive methodology.

Electron−electron interaction error can also be accounted for with the Hubbard U model, which observes rutile−anatase energetic ordering changes over specific ranges of U applied to the 3d orbitals of Ti and gives physical delocalization behavior over the range $U_{Ti,3d}$ = 3.0−4.0 eV.[63] Furthermore, U parameters between 3.0 and 3.5 eV have already been calculated for several TiO_2 polymorphs using the first-principles method of linear response theory,[65−67] illustrating the potential for employing this method to consistently and accurately predict phase stability across broad sets of BO_2 polymorphs.[3,65]

This study will focus on determining the extent to which a consistent relative energetic ordering can be achieved over calculations that vary in functional and pseudopotential selection. Under typical ambient conditions, three naturally occurring TiO_2 polymorphs are expected to occur, namely rutile, anatase, and brookite.[3,11,12,25,47] Rutile has been experimentally shown to be the only naturally occurring stable bulk TiO_2 polymorph;[8,12,25,68] thus, this study will investigate whether DFT can consistently confirm that the rutile → anatase and rutile → brookite formation energies are positive. Additionally, this study will confirm whether DFT can predict a consistent ordering of the metastable TiO_2 polymorphs anatase and brookite, namely $E_{rutile} < E_{anatase} < E_{brookite}$ or $E_{rutile} < E_{brookite} < E_{anatase}$. Though experimental studies have shown that factors such as TiO_2 particle size and synthesis temperature can impact the relative stability of TiO_2 polymorphs that are less thermodynamically accessible than brookite and anatase,[49,50] extensive research on the bulk phase stability of TiO_2 with the application of hydrostatic pressure have shown that the columbite TiO_2 polymorph is the next most accessible phase during compression,[21,29,69−72] decompression,[25,30] or both[68,73] cycles. Therefore, this study will investigate whether the rutile → anatase and rutile → brookite formation energies are consistently less than that of rutile → columbite. Ranges of Hubbard U values[40,58−60] and fractions of exact exchange[61,63] will be applied to DFT calculations to assess the intervals within which consistent relative energetic orderings can be achieved.[63,74] Linear response theory will be applied to determine whether first-principles methods can calculate U values that reliably fall within those intervals *a priori*.[65,75]

METHODOLOGY

Four polymorphic TiO_2 structures were investigated in this study, namely rutile (space group $P4_2/mnm$), anatase (space group $I4_1/amd$), brookite (space group $Pbca$), and columbite (space group $Pbcn$). This study will not focus on the synthetically formed ramsdellite (TiO_2(R)) and hollandite (TiO_2(H)) polymorphs that can be thermodynamically accessible under ambient conditions.[31] Initial input for the atomic positions and lattice parameters of these structures was provided from experimental data.[76] In all calculations involving relative energetic ordering, unit cell representations of the rutile (6 atom), anatase (6 atom), columbite (12 atom), and brookite (24 atom) polymorphs were evaluated. The Birch−Murnaghan equation of state (EOS) was employed to calculate the ground state energies of these systems.[77]

With respect to the Vienna Ab-initio Simulation Package (VASP) calculations[78,79] completed in this study, all pseudopotentials used were generated by the projector augmented wave (PAW)[80] method. Relative energetic ordering was tested using the local density approximation (LDA)[81] exchange-correlation functional and four generalized gradient approximation (GGA) functionals, featuring the Perdew−Burke−Ernzerhof (PBE),[82] Perdew−Burke−Ernzerhof for solids (PBEsol),[83] Armiento−Mattsson (AM05),[84] and Perdew−Wang (PW91)[85] parametrizations. VASP version 5.2.12 was used in all calculations except for those involving the PW91 functionals, which used VASP version 5.3.5.[78,79] Using the PBE functional, five combinations of Ti and O pseudopotentials were investigated in energetic ordering calculations. They are labeled Ti and O (the default pseudopotentials), Ti_pv (treating p electrons as valence electrons) and O, Ti_sv (treating s electrons as valence) and O, Ti_pv and O_s (soft

DOI: 10.1021/acs.jpcc.5b05338
J. Phys. Chem. C 2015, 119, 21060−21071

pseudopotential for oxygen), and Ti_sv and O_s in the VASP software package. Different available PAW pseudopotentials for O, including the harder O pseudopotential (O_h), were not investigated due to the higher required energy cutoffs required by their use.[78,79]

The rotationally invariant Dudarev implementation of the Hubbard U model was used to account for electron−electron interaction error in spin-polarized, paramagnetic (PM) TiO_2 polymorph calculations.[63,86] In this implementation, the on-site Coulombic (U) and exchange (J) terms are combined into a single effective U parameter (U_{eff}) to account for errors in exchange correlation on Ti 3d orbitals.[86] Calculations completed using this procedure in VASP employed a 600 eV plane-wave energy, an 8 × 8 × 8 Monkhorst−Pack[87] k-point sampling mesh set with respect to each TiO_2 unit cell (containing 6, 12, or 24 atoms), and a 0.01 eV/Å force tolerance on each atom.

Corresponding calculations employing the PBE0[88] and HSE06[89,90] hybrid functionals (VASP version 5.2.12) and PAW pseudopotentials were completed for the rutile and anatase TiO_2 polymorphs. Calculations completed using this procedure employed a 550 eV plane-wave energy, a 6 × 6 × 6 Gamma point centered[40] k-point sampling mesh set with respect to each tested TiO_2 unit cell (containing 6 atoms), and a 0.02 eV/Å force tolerance on each atom. Calculation of paramagnetic, first-principles derived Hubbard U values for pertinent TiO_2 polymorph systems is accomplished via implementation of linear response theory in VASP (version 5.3.5).[60,65,91] These linear response calculations demonstrated the effects of varying Ti pseudopotential selection (Ti, Ti_pv, or Ti_sv) and GGA functional parametrization (PBE or PBEsol), employing a 600 eV plane-wave energy cutoff and an 8 × 8 × 8 Monkhorst−Pack[87] k-point sampling mesh set with respect to each TiO_2 unit cell. Different 2 × 2 × 2 supercells were used to perform linear response calculations on rutile (48 atoms), anatase (48 atoms), and columbite (96 atoms) systems, while a 2 × 2 × 1 supercell was applied in corresponding calculations on brookite (96 atoms). These selections were made to balance the computational expense of performing linear response calculations on larger systems with the possible "delocalized background" contributions to calculated U values resulting from the necessary use of finite supercells.[65]

Further information on the procedures used to complete calculations involving U_{eff}, hybrid functionals, and linear response U values, as well as information on structural relaxation approaches used in particular EOS calculations, can be found in the Supporting Information for this study.

RESULTS AND DISCUSSION

The results of evaluating the energetic ordering of rutile, anatase, columbite, and brookite TiO_2 polymorphs as a function of the Hubbard U_{3d} parameter on Ti 3d orbitals are calculated and presented in accordance with several conventions. First, formation energies used to evaluate energetic ordering, which are calculated as the DFT total energy differences between rutile and any other polymorph, are normalized with respect to the TiO_2 formula unit. Second, the ranges of U values over which the relative energetic ordering of stable and metastable bulk TiO_2 polymorphs is consistent with experimental results[8,68] are evaluated over U_{3d} intervals of either 0.0−6.0 or 0.0−9.0 eV in 1.0 eV increments. These intervals are selected due to considerations of energetic ordering switching,[74] electron delocalization,[63,64] and U parameter calculation[66,67] completed in previous literature reports. Third, despite the use of first-principles and experimentally fitted U parameters to the 2p orbitals of O in previous work,[67] U parameters were not applied to these orbitals, as the Hubbard U model can only physically characterize d−d and f−f orbital interactions effectively.[92] Experimental fitting of U values is also not suitable for accurate prediction of energetic properties in different materials sets[3,37] or integration into different first-principles calculations requiring physically realistic input,[54,55] as U values themselves represent intrinsic responses to orbital occupation perturbation.[65,93] Lastly, in order to illustratively compare the relative energetic differences of any set of polymorphs characterized by any sets of functionals or pseudopotentials studied, a graphical visualization procedure is described in the Supporting Information. However, demonstration of the impact of various factors on energetic ordering will be illustrated through several figures within this study. These figures will directly highlight comparisons between GGA (PBE) and LDA functional calculations (Figure 1), PBE functional calculations incorporating Ti p-shell valence inclusive pseudopotentials (Figure 2), PBE functional calculations incorporating Ti s-shell valence inclusive pseudopotentials (Figure 3), and GGA functional calculations of varied (PBEsol, PW91, AM05) parametrization (Figure 4).

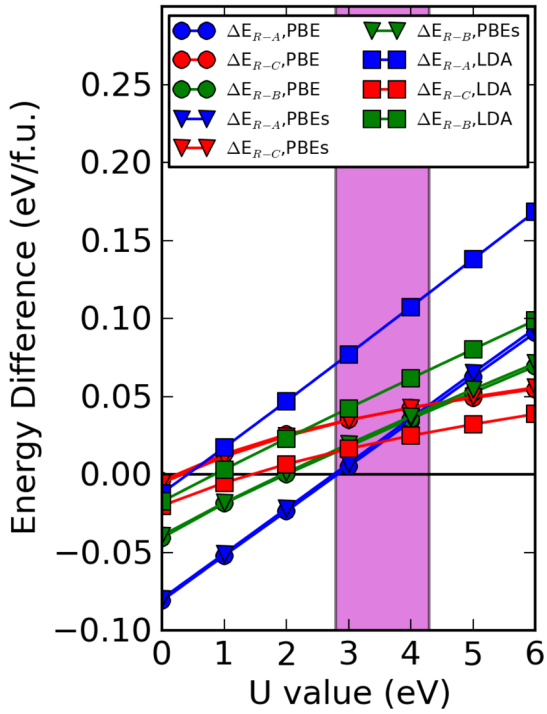

Figure 1. Relative energetic (ΔE) differences between an anatase (A), columbite (C), or brookite (B) polymorph and a rutile (R) polymorph calculated with the same functionals (GGA-PBE or LDA functionals, Ti and O pseudopotentials) and pseudopotential sets (PBE, Ti and O_s). Relative energies, which are all normalized with respect to the TiO_2 three atom formula unit and set with respect to rutile energies for given functional and pseudopotential combinations (black line), represent less stable polymorphs over values of U_{3d} when above the black line. The range of experimentally consistent energetic orderings for all plotted energetic relationships (2.8−4.3 eV) is highlighted by the purple area.

DOI: 10.1021/acs.jpcc.5b05338
J. Phys. Chem. C 2015, 119, 21060−21071

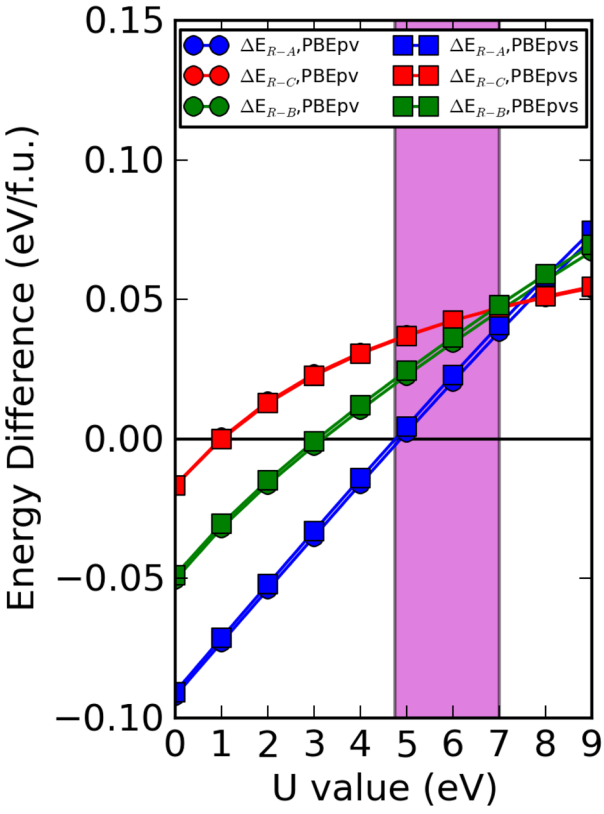

Figure 2. Relative energetic (ΔE) differences between an anatase (A), columbite (C), or brookite (B) polymorph and a rutile (R) polymorph calculated with the same pseudopotential sets (GGA-PBE functionals, Ti_pv and O or Ti_pv and O_s pseudopotentials). Relative energies, which are all normalized with respect to the TiO_2 three atom formula unit and set with respect to rutile energies for given functional and pseudopotential combinations (black line), represent less stable polymorphs over values of U_{3d} when above the black line. The range of experimentally consistent energetic orderings for all plotted energetic relationships (4.7−7.0 eV) is highlighted by the purple area.

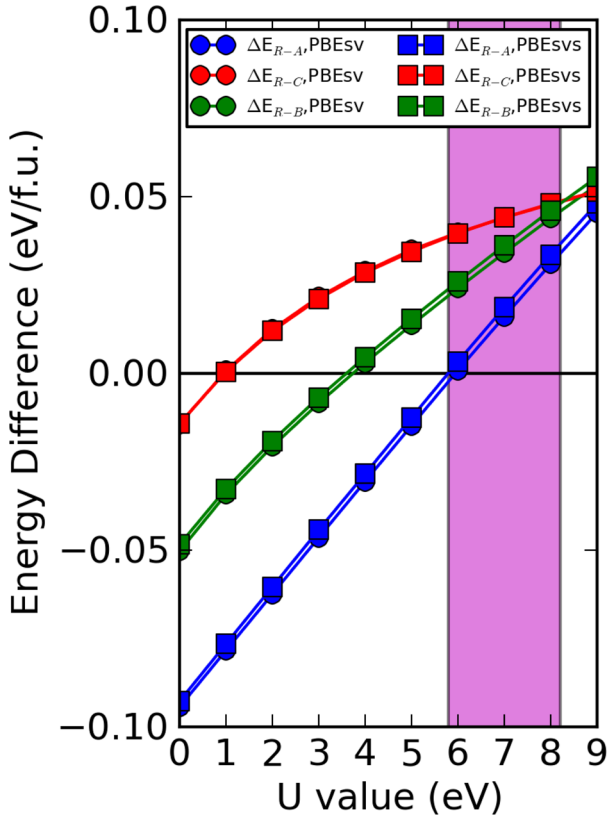

Figure 3. Relative energetic (ΔE) differences between an anatase (A), columbite (C), or brookite (B) polymorph and a rutile (R) polymorph calculated with the same pseudopotential sets (GGA-PBE functionals, Ti_sv and O or Ti_sv and O_s pseudopotentials). Relative energies, which are all normalized with respect to the TiO_2 three atom formula unit and set with respect to rutile energies for given functional and pseudopotential combinations (black line), represent less stable polymorphs over values of U_{3d} when above the black line. The range of experimentally consistent energetic orderings for all plotted energetic relationships (5.8−8.2 eV) is highlighted by the purple area.

Effects of Pseudopotentials. As is shown in Figure 1, the use of softer O pseudopotentials (O_s) on calculations employing the PBE functional has little effect on energetic ordering predictions, which successfully find rutile to be the most energetically favorable polymorph above approximately U_{3d} = 2.8 eV, brookite to be more stable than rutile above approximately U_{3d} = 2.0 eV, anatase to be less stable than rutile and consistently more stable than brookite between approximately U_{3d} = 2.8−4.0 eV, and columbite to be the least stable polymorph between approximately U_{3d} = 0.3−4.3 eV. Therefore, in an approximate range of U_{3d} = 2.8−4.3 eV, all experimentally expected results for energetic ordering criteria are met. In contrast, use of the LDA functional shows rutile to be the most energetically favorable polymorph above approximately U_{3d} = 1.5 eV, brookite to always be more stable than anatase though less stable than rutile above approximately U_{3d} = 0.9 eV, and anatase to be less stable than rutile and brookite above approximately U_{3d} = 0.4 eV. However, columbite is never predicted to be the least energetically stable of the four phases at any tested U_{3d} value when using the LDA functional. Therefore, LDA is not capable of entirely resolving experimentally consistent relative energetic stability upon applying any single value of U_{3d} to all tested TiO_2 polymorphs.

Comparison of brookite and columbite results achieved with different functionals reveals that—with respect to the PBE functional phase lines of varying U_{3d} parameter magnitude in Figures 1, 2, 3, and 4—the relative formation energy of LDA functional resolved brookite increases and columbite decreases. Nevertheless, the largest change in LDA functional results is seen in the large upward shift of the relative formation energetics of anatase. Figures 2 and 3, which incorporate p-shell and s-shell valence inclusive Ti pseudopotentials and O pseudopotentials of varying softness, demonstrate similar energetic behavior. In both figures, which feature four pseudopotential combinations, columbite is the least stable polymorph above approximately U_{3d} = 1.0 eV and brookite is the next least stable between approximately U_{3d} = 3.1−7.0 eV. However, the relative energetics of the p-shell valence inclusive Ti pseudopotential calculations show that anatase is unphysically more stable than rutile at U_{3d} values less than 4.7 eV, whereas the analogous change in energetic favorability occurs at approximately U_{3d} = 5.8 eV in calculations featuring s-shell valence inclusive Ti pseudopotentials.

With respect to the value of U_{3d} at which rutile−anatase energetic ordering changes, these two sets of calculations are more consistent with previously derived results.[74] Overall, the results analyzed thus far indicate that for all VASP calculations incorporating the PBE parametrization of the GGA functional in accompaniment with varied types of Ti and O

DOI: 10.1021/acs.jpcc.5b05338
J. Phys. Chem. C 2015, 119, 21060−21071

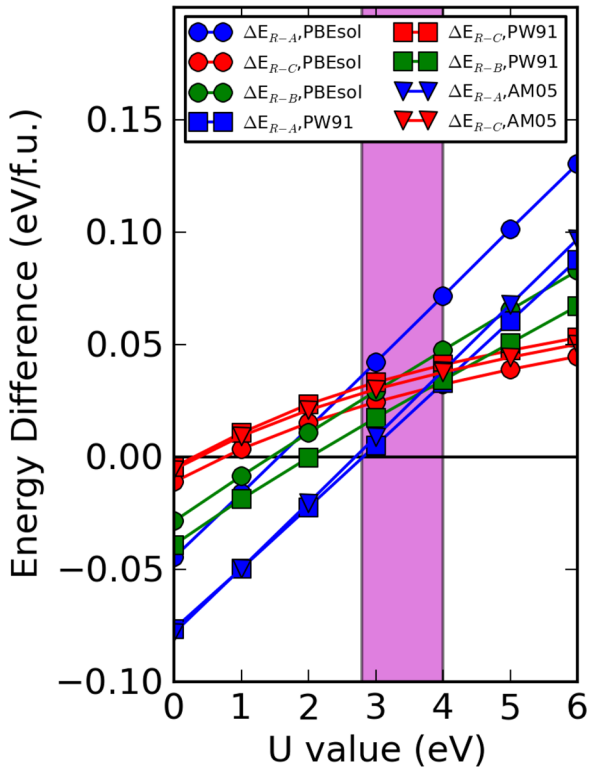

Figure 4. Relative energetic (ΔE) differences between an anatase (A), columbite (C), or brookite (B) polymorph and a rutile (R) polymorph calculated with the same functional parametrizations (GGA functional with PBEsol, PW91, and AM05 parametrizations, Ti and O pseudopotentials). Relative energies, which are all normalized with respect to the TiO_2 three atom formula unit and set with respect to rutile energies for given functional and pseudopotential combinations (black line), represent less stable polymorphs over values of U_{3d} when above the black line. The range of experimentally consistent energetic orderings for all plotted energetic relationships (2.8−4.0 eV) is highlighted by the purple area.

pseudopotentials, there exists a pseudopotential-dependent U_{3d} range at which the polymorph energetic ordering $E_{rutile} < E_{anatase} < E_{brookite} < E_{columbite}$ is maintained. In Figures 2 and 3, an energetic ordering consistent with experimental results, namely $E_{rutile} < E_{anatase} < E_{brookite} < E_{columbite}$, is respectively maintained within the intervals 4.7−7.0 and 5.8−8.2 eV. These U_{3d} ranges are largely maintained regardless of whether soft (O_s) or standard (O) oxygen pseudopotentials are used.

Effects of Exchange-Correlation Functionals. As shown in Figure 4, the relative energetics of several sets of calculations involving different types of GGA functionals consistently reveal ranges of U_{3d} over which the $E_{rutile} < E_{anatase} < E_{brookite} < E_{columbite}$ energetic ordering is preserved. In this figure, results for the TiO_2 brookite polymorph featuring use of the AM05 functional were omitted due to convergence issues. In the case of PW91 and AM05 functionals, anatase becomes more stable than rutile at around U_{3d} = 2.7 or 2.8 eV, respectively, and remains less favorable than columbite until approximately 4.3 or 4.0 eV, respectively. In the case of the PBEsol functional, an upward shift in the relative energy of anatase (with respect to that of rutile) causes anatase to become more favorable than rutile at around U_{3d} = 1.6 eV and less favorable than columbite at approximately U_{3d} = 2.1 eV. While PW91 brookite becomes more favorable than rutile above approximately U_{3d} = 2.0 eV and stays less favorable than anatase below approximately U_{3d} = 4.0 eV, PBEsol brookite becomes more favorable than rutile at approximately U_{3d} = 1.5 eV though remains less favorable than columbite until U_{3d} = 2.4 eV largely due to the increased formation energy values of anatase.

Similarly, PW91 and AM05 columbite are the least energetically favorable polymorphs within their functionals in the approximate range of U_{3d} = 0.4−4.1 or 0.4−4.3 eV, respectively, while PBEsol columbite is least favorable within the narrower U_{3d} = 0.8−2.1 eV range. Thus, all VASP calculations incorporating GGA functionals preserve the $E_{rutile} < E_{anatase} < E_{brookite} < E_{columbite}$ energetic ordering within ranges of U_{3d} values on Ti, the breadth of which is most likely and prominently impeded by underestimation of the stability of anatase relative to rutile. The data sets featuring the PBEsol GGA (Figure 4) and LDA (Figure 1) functionals most prominently illustrate this characteristic. Over all values of U_{3d}, these figures also consistently illustrate a slighter increase in the relative formation energy of brookite and a comparable decrease in the relative formation energy of columbite. However, the magnitudes of these shifts in formation energy trends are only capable of impacting the size of the U_{3d} range in which the $E_{rutile} < E_{anatase} < E_{brookite} < E_{columbite}$ energetic ordering exists, instead of entirely precluding the existence of such a U_{3d} range.

As was observed in previous research for the LDA functional[46] and shown above for LDA and PBEsol functionals, a consistent shift of the rutile−anatase relative energetic trend occurs for all values of U tested. Previous research has indicated that functional selection has demonstrated little effect on calculated TiO_2 rutile and anatase band gaps[74,94] and that cell volumes for matching systems have been shown to be consistently lower when applying PBEsol and LDA functionals than PBE functionals.[37] Therefore, the constant energetic shifts of LDA and PBEsol rutile−anatase energetic trends appear to be linked to changes in equilibrium volume rather than electronic structure. In contrast, electronic structure features such as band gap have been proposed to be more directly linked to U parameters placed on the 2p orbitals of O anions rather than the 3d orbitals of Ti cations in TiO_2, as the application of high magnitude $U_{3d,Ti}$ values needed to reproduce experimental band gaps does not reproduce physical vacancy defect states.[95,96] With respect to previous first-principles research concerning first-principles rutile[74,97] and anatase[98,99] electronic structure calculations, the changing of rutile−anatase energetic ordering across these energetic trends appears to be most strongly related to the narrowing and upward contraction of Ti 3d conduction band densities of state with the increase of $U_{3d,Ti}$. A comparison between bulk rutile[97] and anatase[99] band structures reveals that with respect to their corresponding GGA electronic structures the contribution of comparable values of $U_{3d,Ti}$ to both polymorphs disproportionately changes the differences between their conduction band (CB) minima and valence band (VB) maxima. Thus, this disproportionality between changes in the CB−VB differences of rutile and anatase with the incrementation of U, which features greater increases in the CB−VB difference of rutile with increasing U resulting from a more pronounced contraction of the Ti 3d states occupying its CB minima, serves to possibly indicate a physical link between changes in rutile−anatase relative energetic ordering and the corresponding electronic structures of rutile and anatase.[74]

Linear Response *U*. In order to evaluate the extent to which relative TiO_2 polymorph energetics can be predicted, the

DOI: 10.1021/acs.jpcc.5b05338
J. Phys. Chem. C 2015, 119, 21060−21071

linear response method[65,75] is employed to calculate the first-principles values of the Hubbard U applied to all Ti cations in each system. In past research, a significant range of first-principles calculated U values have been resolved for rutile TiO_2 polymorph systems, namely those studied to evaluate different properties of interest. For example, a $U_{3d,Ti}$ value of 0.15 eV was achieved and applied to calculations improving TiO_2 band gap estimation relative to experimentally calculated values,[96] while a corresponding value of 4.95 eV was achieved and implemented in calculations comparing large sets of surface adsorption energetics to matching oxygen evolution reaction (OER) activity trends.[100] Furthermore, application of the self-consistent extension[75] of the linear response approach to comparatively model intrinsic defect behavior in TiO_2 rutile and anatase achieved respective first-principles resolved U values of 3.23 and 3.25 eV for each system.[67]

As shown in Table 1, the U values achieved in this study are not only comparable to several previously calculated values but also illustrate possible reasons for differences in those previously calculated U values. When applying the PBE functional parametrization and the p-valence inclusive Ti pseudopotential to the linear response calculation of $U_{3d,i}$ for rutile in VASP, a U value of 4.773 ± 0.267 eV is resolved. This result, which is consistent with that achieved by Xu et al. (4.95 eV) within uncertainty,[100] was obtained in Quantum Espresso (QE)[101] while using the same functional as that applied in Xu et al. and a semicore p-valence state inclusive, Ultrasoft, GBRV Ti pseudopotential featuring a nonlinear core correction.[102] Similarly, applying the PBE functional parametrization and a standard pseudopotential in VASP calculations yields a result of 3.102 ± 0.137 eV, which is equivalent to the QE resolved result shown in Mattioli et al. (3.23 eV) within uncertainty.[67] This result from Mattioli et al. was achieved while also using the PBE functional and a highly similar Ultrasoft pseudopotential, which differs from its GRBV analogue predominately in its lack of nonlinear core correction.[101,103] Despite the difference in the software package used to calculate U value results in this paper (VASP) and past research (QE), strong similarity between the effects of implementing p-valence inclusive Ti pseudopotentials in VASP and including a nonlinear core correction in a semicore valence state inclusive Ti pseudopotential in QE is evident. Thus, when considering the effects of pseudopotential selection on TiO_2 polymorph linear response U calculation independent of other factors, the use of pseudopotentials that include core states in their valence configurations apparently and systematically increases the values of calculated U results.

Table 1. Linear Response Calculated U Parameter Values Corresponding to the 3d Orbitals of Ti Cations, Distinguished by the Functionals and Pseudopotentials Used To Calculate Them[a]

polymorph	functional	pseudopotentials	U (eV)
rutile	PBE	Ti, O	3.102 ± 0.137
anatase	PBE	Ti, O	2.929 ± 0.133
columbite	PBE	Ti, O	2.983 ± 0.137
brookite	PBE	Ti, O	2.934 ± 0.128
rutile	PBEsol	Ti, O	2.727 ± 0.120
anatase	PBEsol	Ti, O	2.558 ± 0.117
rutile	PBE	Ti_pv, O	4.773 ± 0.267
anatase	PBE	Ti_pv, O	4.295 ± 0.243
rutile	PBE	Ti_sv, O	6.030 ± 0.392
anatase	PBE	Ti_sv, O	5.321 ± 0.370

[a]Uncertainties and sigificant figures are resolved via error propagation methods corresponding to the reported measurement precision of orbital occupations (±0.001) on the perturbed cation.

The extent to which this increase in calculated U values affects all considered polymorphs is additionally illustrated in Table 1, as rutile U values largely uniformly increase from 3.102 eV to 6.030 or 4.773 eV in the cases of s-valence and p-valence inclusive pseudopotentials, respectively. Anatase U values also largely uniformly increase from 2.929 eV to either 4.295 or 5.321 eV for p-valence and s-valence inclusive pseudopotentials, respectively. Consideration of the rutile−anatase relative formation energy U range results derived in past research[74] or formerly in this study, in conjunction with the established link between pseudopotential selection and U value, reveals that both U values and their associated formation energies increase proportionately with changes in pseudopotential selection. In the case of changing from standard to p-valence or s-valence inclusive Ti pseudopotentials in rutile-based calculations, changes in U values and experimentally consistent U ranges are equivalent and energetic ordering predictions are conserved within uncertainty as pseudopotentials are changed. However, this does not occur in the case of p-valence and s-valence inclusive pseudopotentials for anatase-based calculations. In this case, p-valence and s-valence anatase-based calculations would require U values and associated uncertainties that respectively spanned ranges encompassing 4.7 and 5.8 eV, though Table 1 indicates that this is only true for rutile-based calculations. A possible explanation for this inequivalence of U value and U range changes when assessing the anatase polymorph is proposed in the Supporting Information.

In contrast to changes in pseudopotential selection, changing the functional from PBE to PBEsol while maintaining standard pseudopotential selection does not cause a proportional, joint shift of calculated U values and experimentally consistent U ranges. This results from the nonsystematic upward shift observed by the rutile−anatase formation energy curve, as is shown in Figure 4. Though both rutile and anatase calculated U values decrease significantly when considering PBEsol functional results (with respect to PBE results) within uncertainty, neither polymorph U value spans the narrow 1.5−2.1 eV U range within which experimental energetic ordering consistency is achieved. Results employing the PBE functional and standard pseudopotentials are available for all four studied polymorphs. Within uncertainty, each of their U values is explicitly above 2.8 eV and below 4.3 eV. Thus, in accordance with the U ranges visualized in Figure 1, these calculated U results indicate that the energetic ordering of all four polymorph systems is necessarily experimentally consistent via the relationship $E_{rutile} < E_{anatase} < E_{brookite} < E_{columbite}$. Additionally, within uncertainty, all four polymorphs share a common set of U values through which they can be directly energetically compared.

Impact of Hybrid Functionals and Fraction of Exact Exchange. The use of different functionals has been shown to impact predictions of possible energetic ordering in stable, metastable, and unstable TiO_2 polymorphs, particularly affecting the rutile−anatase relative formation energy trend while varying U_{3d}. In past research, varying the U_{3d} on Ti 3d orbitals as a tunable parameter over ranges comparable to 2.8−4.3 eV, namely the range shown capable of achieving experimentally consistent energetic ordering previously, has been demonstrated to affect the physicality of electron localization on those Ti 3d orbitals.[63,64] Hybrid functionals

DOI: 10.1021/acs.jpcc.5b05338
J. Phys. Chem. C 2015, 119, 21060−21071

have been shown capable of affecting the relative energetic ordering of rutile and anatase to the possible extent of reversing their ordering.[62] Proposals of the relationship between variation in the fraction of exact exchange contributed to a hybrid functional and the relative localization of valence (3d) electrons on Ti cations[63,64] and in general applications[61] have been made in past research. Considering that achieving physical electron localization behavior on Ti cations has been demonstrated possible by tuning either U_{3d} in Hubbard U calculations or the fraction of exact exchange in hybrid functional calculations,[63,64] a rutile−anatase relative formation energy consistent with experimental expectations should be achievable within a range of either U_{3d} values or fractions of exact exchange.

In accordance with the calculation of U_{3d} intervals containing an experimentally consistent rutile−anatase energetic ordering, Figure 5 illustrates the fractions of exact exchange contributed

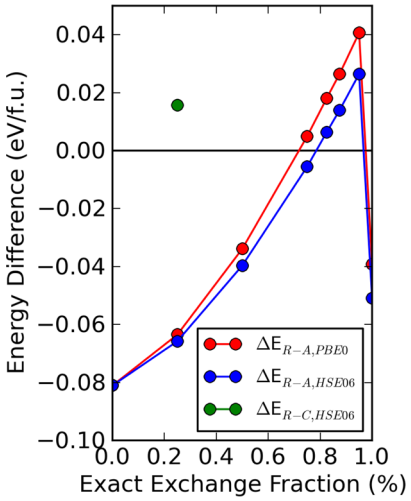

Figure 5. Relative energetic (ΔE) differences between an anatase (A) or columbite (C) and a rutile (R) polymorph calculated using the PBE0 and HSE06 hybrid functionals and standard Ti and O pseudopotentials. Relative energies, which are all normalized with respect to the TiO_2 three atom formula unit and set with respect to rutile energies for given functionals (black line), represent less stable polymorphs over fractions of HF exact exchange when above the black line.

to the PBE0 and HSE06 hybrid functionals in order to achieve $E_{rutile} < E_{anatase}$. When reviewed over several fractions of exact exchange (a = 0.00, 0.25, 0.50, 0.75, 0.825, 0.875, 0.95, and 1.00),[88,89] the PBE0 and HSE06 hybrid functionals both initially observe a monotonic upward trend when increasing the fraction of exact exchange, starting at a shared relative rutile−anatase formation energy of approximately −0.081 eV/TiO_2. Energetic ordering changes from $E_{anatase} < E_{rutile}$ to $E_{rutile} < E_{anatase}$ occur for the PBE0 hybrid functional at approximately a = 0.72 and occur for the HSE06 hybrid functional at approximately a = 0.78. As further detailed in the Supporting Information, these monotonic increases in rutile−anatase relative formation energy appear to occur until the limit of HF exact exchange is reached.

For the HSE06 and PBE0 functionals, formation energy peaks are separated by approximately 0.015 eV/TiO_2, with PBE0 having a higher peak located between 0.040 and 0.045 eV/TiO_2. A more exact interpolation of the points at which the rutile−anatase relative formation energy peaks and reverts back to $E_{anatase} < E_{rutile}$ is impaired by both the narrowness of the range of a over which the monotonic decline in formation energy is observed and the low number of data points resolved within that range. Despite the achievement of an experimentally consistent reversal in the rutile−anatase relative energetic ordering at higher fractions of HF exact exchange, improvement of the exact exchange fraction in Lee, Yang, and Parr (LYP) parametrized hybrid functionals from 20% (B3LYP or Becke, three parameter, Lee−Yang−Parr) to 50% (H&HLYP or Half and Half, Lee−Yang−Parr) led to the calculation of physically unrealistic electronic structures in rutile and anatase TiO_2.[63,64] Therefore, even though the improvement of exact exchange fraction in hybrid functionals can lead to experimentally consistent energetics in BO_2 systems, the physicality of the electronic structure yielding those structures cannot be guaranteed using solely hybrid functional energetic calculations.

Despite the evidence of consistent change in Ti 3d electron localization and delocalization behavior with the incrementation of U_{3d} value or exact exchange fraction (a),[61,63] the rutile−anatase relative formation energy trend is clearly not monotonic over all values of the exact exchange fraction. Therefore, electron localization on Ti 3d orbitals cannot be the only factor impacting relative formation energetics in rutile and anatase polymorphs. The short-range, long-range (SR-LR) separation parameter (ω = 0.2) of the HSE06 hybrid functional,[89] which distinguishes it from the related PBE0 functional, defines the long-range distance after which HF exchange is replaced with PBE exchange in these calculations. This replacement of exchange has clear effects on the relative rutile−anatase energetics when considering that the range in which HSE06 achieves $E_{rutile} < E_{anatase}$ is significantly narrower than that of PBE0, while the interpolated peak of the monotonic increase in HSE06 is also significantly lower than that of PBE0. Though the removal of long-range HF exchange clearly affects energetics, this contribution to energetics is insufficient to prevent the rutile−anatase energetic ordering change, as both PBE0 and HSE06 feature a rutile−anatase energetic ordering change.

Further analysis of data involving several features linked to the nonmonotonic trend formed by varying the fraction of HF exchange are developed in the Supporting Information for this study. For both polymorphs in both hybrid functionals tested, a summary of these results reveals that the inversely proportional relationship between rutile and anatase cell volumes and the rutile−anatase formation energy is very strong, illustrating that an analogue of the relationship between atomic structure and relative energetics found when varying U in Hubbard U calculations is also present when varying the HF exchange fraction in hybrid functional calculations.[103,104] In the case of rutile, cell volume first decreases in proportion with the initial monotonic trend in relative formation energy and then increases upon reversal of the trend, yielding system volumes at the HF exact exchange limit (a = 1.0) that vary across tested functionals. In the case of anatase, the same increasing and decreasing trends in cell volume are present, though the system volume at the HF exact exchange limit more consistently matches that observed when a = 0.25 for both PBE0 and HSE06 functionals.

When reviewing contributions to the expansion and contraction of the rutile and anatase unit cells with the addition of HF exchange across both hybrid functionals, a component of cell volume that changes highly proportionately with rutile−anatase formation energetics is the c/a ratio of

DOI: 10.1021/acs.jpcc.5b05338
J. Phys. Chem. C 2015, 119, 21060−21071

rutile. A similar level of proportionality can be observed in comparing the relationship between the c/a ratio of anatase and HF exchange fraction with the relationship between corresponding anatase cell volumes and HF exchange fractions. In these relationships, which are depicted in the Supporting Information, all volumetric information is normalized with respect to the volumetric datum possessing the lowest HF exchange fraction in each plot. This normalization, which is accomplished for each system and each material property plotted, facilitates the direct comparison of different systems and reveals the apparent proportional relationships shared by different systems across the same property. In both proportional relationships, the nonmonotonicity originally observed in the rutile−anatase formation energy trend as $a \rightarrow 1$ is observed, namely as a discontinuity of decreasing magnitude in the c/a ratio of rutile and one of increasing magnitude in the c/a ratio of anatase, the cell volume of rutile and the cell volume of anatase. Therefore, the discontinuity observed in formation energy can be strongly linked to variations in multiple structural properties independent of long-range exchange interaction screening, inferring that the physicality of the energetic discontinuity can be more directly determined via comparisons between the structural features yielded from experimental results and first-principles calculations.

In connection with the discontinuity shared by rutile−anatase formation energetics and the c/a ratio trends of rutile and anatase that both vary with HF exchange fraction, continuous portions of those trends share common characteristics. These shared characteristics include the direct relationship between the c/a ratio of rutile and the rutile−anatase formation energy as a function of exact HF exchange, in addition to the inverse relationship between the corresponding c/a ratio of anatase and that formation energy. These relationships directly relate the rutile−anatase formation energy with relative changes in c-axis length for rutile and a-axis length for anatase. When considering previous conclusions stating that electron localization on Ti 3d orbitals cannot be the only factor influencing rutile−anatase formation energetics and that neglecting to consider long-range exact exchange interactions in HSE06 was not sufficient to change relative energetic ordering, the possible link between short-range interactions and changes in the lengths of the shorter axes of both tetragonal polymorphs with corresponding changes in rutile−anatase relative energetic ordering can be developed. Previous research indicates that van der Waals dispersion interactions, which are accounted for by short-range energetic contributions proportional to r^{-6} (r represents interatomic distances), are expected to occur in TiO_2 rutile, anatase, and other polymorphs.[57,105] Given the poor overlap between TiO_2 rutile and anatase experimental cell volumes and cell volumes with experimentally consistent energetic ordering shown in the Supporting Information,[37] the introduction of both short-range dispersion and electron−electron interaction corrections to simultaneously achieve experimentally consistent energetic and structural information on improved accuracy is strongly supported by analysis completed in this research.

Given the connection between structure and rutile−anatase formation energetics in TiO_2 polymorphs, the calculation of formation energetics in similarly structured BO_2 polymorphs using hybrid functionals can also be affected by discontinuities, especially when considering the small magnitude of relative energetic changes resulting from variation in U or a for TiO_2 polymorphs. When measuring the maximum error that can result from using a PBE or HF nonhybridized functional rather than a hybrid functional, the HF exchange fraction of which is set with respect to the interpolated maximum of each formation energy trend ($a \rightarrow 1$), the relative energetic differences between the results produced by either the HSE06 or PBE0 functional with $a \rightarrow 1$ and corresponding results produced via a nonhybridized PBE or HF functional range from 0.068 to 0.127 eV/TiO_2. As shown in the Supporting Information and previous research,[37] epitaxial stabilization of similarly composed polymorphs occurs within an energetic window of 0.1−0.2 eV. Considering that the maximum error reported previously observes the same order of magnitude of the energetic window implemented in epitaxial stabilization applications, the *a priori* use of hybrid functionals as a predictive tool capable of materials selection in these applications is questionable.

CONCLUSIONS

In this study, the relative energetic ordering of rutile, anatase, brookite, and columbite TiO_2 polymorphs has been assessed using DFT+U and hybrid functional methodologies. The relative formation energies of anatase, brookite, and columbite with respect to rutile were evaluated over variation in the U_{3d} parameter on Ti in Hubbard U calculations and the fraction of exact exchange in PBE0 and HSE06 calculations. Past research not incorporating Hubbard U or hybrid functional methodologies of these TiO_2 polymorphs has indicated that their energetic ordering varies with functional selection.[37] However, when incorporating a Hubbard U methodology, energetic trends resulting from variation in U are able to clearly resolve an energetic ordering consistent with experiment that persists regardless of the GGA-based functionals or pseudopotentials employed. In addition to using the LDA functional, this evaluation was completed using the GGA-based functionals PBE, PBEsol, AM05, and PW91. Also, multiple permutations of the s-valence inclusive Ti (Ti_{sv}), p-valence inclusive Ti (Ti_{pv}), soft O (O_s), standard Ti (Ti), and standard O (O) pseudopotentials were considered in this evaluation. Relative energetic orderings consistent with experimental expectations included $E_{rutile} < E_{anatase} < E_{brookite} < E_{columbite}$, $E_{rutile} < E_{brookite} < E_{anatase} < E_{columbite}$, or $E_{rutile} < E_{anatase} < E_{columbite}$.[25,68]

When applying the PBE, AM05, and PW91 functionals in accompaniment with standard or O_s pseudopotentials, an interval of U values between approximately 2.8 and 4.0 eV demonstrated relative energetic ordering consistent with experiment for all polymorphs studied. Inclusion of the Ti_{pv} or Ti_{sv} pseudopotentials on PBE calculations preserved an interval of energetic ordering consistent with experiment that was qualitatively similar to those achieved using standard pseudopotentials. However, in the cases of Ti_{pv} and Ti_{sv} inclusive calculations, these energetic orderings differed from their PBE analogues largely by being shifted rightward with respect to them, as these qualitatively consistent energetic intervals occurred at U = 4.7−7.0 and 5.8−8.2 eV, respectively. As a predominant result of upward shifts of the rutile−anatase energetic trends within them, the PBEsol functional with standard pseudopotentials observed an energetic ordering consistent with experiment within the U interval of 1.5−2.1 eV, whereas the LDA functional did not produce an experimentally consistent energetic ordering at any value of U.

First-principles derived values of U, which have been achieved from linear response theory calculations performed in this study and past research,[67,100] were applied to determine whether experimentally consistent relative energetic ordering

DOI: 10.1021/acs.jpcc.5b05338
J. Phys. Chem. C 2015, 119, 21060−21071

can be predicted in TiO_2 polymorphs. Application of either the first-principles derived U values from this work or corresponding results from other research[67,100] indicates that experimentally consistent results can at least be achieved with the PBE, AM05, and PW91 functionals accompanied by standard pseudopotentials. In past research,[63,67] an approximate U value of 3 eV has been assigned to rutile and anatase polymorph Ti cations to improve the physicality of electronic structure properties relative to experimental results. Application of this U value, or corresponding values calculated via linear response, to the rutile−anatase formation energy reveals a result within the range of 0.00 and 0.01 eV/TiO_2, which is in strong quantitative agreement with past experimental results.[74,106]

The rutile−anatase relative formation energy, which was most responsible for inconsistencies in relative energetic ordering predictions across functionals, was more extensively analyzed using hybrid functional calculations, namely by calculating formation energy as a function of exact exchange using both the PBE0 and HSE06 hybrid functionals. For PBE0 and HSE06 functionals, experimentally consistent $E_{rutile} < E_{anatase}$ energetic ordering was achieved at fractions of exact exchange of approximately 0.72 and 0.78, respectively, indicating that controlling the charge localization and delocalization in Ti 3d orbitals can produce experimentally consistent energetics. However, in the limit of 100% exact HF exchange, rutile−anatase energetic ordering was shown to revert to an experimentally inconsistent energetic ordering. For both TiO_2 rutile and anatase, structural features observed strong inverse or direct relationships with formation energetics. Given these connections between structure and energetics and the relative energetic error associated with the inability to select a single fraction of exact exchange for both rutile and anatase predictively, the arbitrary selection of an exact exchange fraction has greater implications on the prediction of relative energetics in generalized BO_2 systems using hybrid functionals. In combination with the absence of a methodology for predicting a suitable fraction of exact exchange for particular sets of TiO_2 polymorphs, the errors in relative energetic ordering resulting from the use of hybrid functionals on TiO_2 polymorphs suggest care should be taken in their use in predicting relative energetics in less studied BO_2 systems. Minimally, these predictive calculations could require the use of a high fraction of exact exchange not equal to the HF limit to accommodate relative formation energetics similar to the rutile−anatase energy, though exact magnitudes of exact exchange cannot be prescribed based on this study of TiO_2 polymorphs.

In each case of varied pseudopotential and functional selection evaluated in this study for Hubbard U and hybrid functional inclusive calculations, the quantitative differences between the relative energetics of distinct TiO_2 polymorphs, namely energetics contained by the prescribed ranges of linear response calculated U or experimentally consistent energetic ordering, are generally within a range of 0.1 eV of one another. Despite the low magnitude of these energetic differences, the addition of a constant U = 3 eV to the 3d orbitals of Ti cations has been demonstrated to predict experimentally consistent energetic ordering within the measurement uncertainty associated with U calculations. Though relative energetic results resolved in this study are most directly related to internal energy[100] or formation enthalpy values achieved while neglecting pressure involved contributions,[58,74] the consideration of energetic contributions beyond those resolved in first-principles ionic and electronic relaxation calculations is required when applying the BO_2 relative energetics yielded in this study to corresponding Gibbs free energy calculations.[107] Previous information has shown that the consideration of entropy contributions over a wide range (0−1300 K) of temperatures does not affect rutile−anatase energetic ordering, as the magnitude of the standard entropy of formation of rutile is strictly greater than that of anatase over the evaluated temperature range.[108] Past research evaluating the zero-point energy vibrational contributions of TiO_2 rutile and anatase, which was calculated at U = 0 eV, reveals an approximate difference of 0.02 eV between the two contributions that favors stabilizing anatase.[109,110] Nevertheless, the calculation of vibrational contributions at finite temperatures using phonon densities of state (also at U = 0 eV) reveals, in accompaniment with corresponding experimental data, that a TiO_2 rutile−anatase phase transformation occurs between 1200 and 1340 K.[32] Though both experimental and computational results imply that vibrational contributions could affect relative energetic ordering in calculated Gibbs free energy results at higher temperatures, these vibrational effects are not anticipated to stabilize anatase relative to rutile in DFT calculations and under experimental conditions not involving elevated temperature and pressure conditions.

Recent efforts have been made in the determination of distinct exact exchange fractions suitable for the calculation of properties in individual systems by comparing GW self-energy calculation contributions to those of hybrid functionals, namely via relating the inverted dielectric matrix of the screened nonlocal exchange term of the GW calculation to the fraction of exact HF exchange contributed to hybrid functional calculations.[105,111] Despite the largely experimentally consistent results achieved when extending this approach to compute a pair of related reaction energies involving two systems (the TiO_2 rutile polymorph and the Ti_2O_3 corundum polymorph) that each possessed a distinct, calculated fraction of exact exchange, the application of this approach to the relative formation energies involving rutile, anatase, and brookite TiO_2 polymorph pairs yielded an experimentally inconsistent energetic ordering ($E_{anatase} < E_{brookite} < E_{rutile}$).[105] Nevertheless, appropriate application of the Hubbard U method and self-consistent linear response theory enables consistent, precise prediction of experimental energetic orderings of TiO_2 polymorphs and related systems, encouraging the use of Hubbard U methodologies to predict relative energetic ordering in less studied BO_2 systems.

■ ASSOCIATED CONTENT

Supporting Information

The Supporting Information is available free of charge on the ACS Publications website at DOI: 10.1021/acs.jpcc.5b05338.

A complete database of the results from this work with examples of using the data to generate the figures (PDF)

■ AUTHOR INFORMATION

Corresponding Author

*Phone 412-268-7803; Fax 412-268-7139; e-mail jkitchin@andrew.cmu.edu (J.R.K.).

Notes

The authors declare no competing financial interest.

DOI: 10.1021/acs.jpcc.5b05338
J. Phys. Chem. C 2015, 119, 21060−21071

■ ACKNOWLEDGMENTS

The authors of this paper thank Dr. Giuseppe Mattioli for his contributions to discussions involving the use of the Hubbard *U* method in this article. The computing resource used to complete this paper was provided by Carnegie Mellon University and its Department of Chemical Engineering. J.R.K. gratefully acknowledges partial support from the DOE Office of Science Early Career Research program (DE-SC0004031).

■ REFERENCES

(1) Francisco, M. S. P.; Mastelaro, V. R.; Nascente, P. A. P.; Florentino, A. O. Activity and Characterization By XPS, HR-TEM, Raman Spectroscopy, and BET Surface Area of CuO/CeO_2-TiO_2 Catalysts. *J. Phys. Chem. B* **2001**, *105*, 10515−10522.

(2) Bokhimi, X.; Zanella, R. Crystallite Size and Morphology of the Phases in Au/TiO_2 and Au/Ce-TiO_2 Catalysts. *J. Phys. Chem. C* **2007**, *111*, 2525−2532.

(3) Hamad, B. A. First-Principle Calculations of Structural and Electronic Properties of Rutile-Phase Dioxides (MO_2), M = Ti, V, Ru, Ir and Sn. *Eur. Phys. J. B* **2009**, *70*, 163−169.

(4) Nakata, K.; Fujishima, A. TiO_2 Photocatalysis: Design and Applications. *J. Photochem. Photobiol., C* **2012**, *13*, 169−189.

(5) Indrakanti, V. P.; Kubicki, J. D.; Schobert, H. H. Photoinduced Activation of CO_2 on Ti-Based Heterogeneous Catalysts: Current State, Chemical Physics-Based Insights and Outlook. *Energy Environ. Sci.* **2009**, *2*, 745−758.

(6) Osterloh, F. E. Inorganic Materials As Catalysts for Photochemical Splitting of Water. *Chem. Mater.* **2008**, *20*, 35−54.

(7) Man, I. C.; Su, H.-Y.; Calle-Vallejo, F.; Hansen, H. A.; Martínez, J. I.; Inoglu, N. G.; Kitchin, J.; Jaramillo, T. F.; Nørskov, J. K.; Rossmeisl, J. Universality in Oxygen Evolution Electrocatalysis on Oxide Surfaces. *ChemCatChem* **2011**, *3*, 1159−1165.

(8) Hu, Y.-S.; Kienle, L.; Guo, Y.-G.; Maier, J. High Lithium Electroactivity of Nanometer-Sized Rutile TiO_2. *Adv. Mater.* **2006**, *18*, 1421−1426.

(9) Subasri, R.; Deshpande, S.; Seal, S.; Shinohara, T. Evaluation of the Performance of TiO_2-CeO_2 Bilayer Coatings As Photoanodes for Corrosion Protection of Copper. *Electrochem. Solid-State Lett.* **2006**, *9*, B1−B4.

(10) Velichenko, A.; Knysh, V.; Luk'yanenko, T.; Danilov, F.; Devilliers, D. PbO_2-TiO_2 Composite Electrodes. *Prot. Met. Phys. Chem. Surf.* **2009**, *45*, 327−332.

(11) Diebold, U. The Surface Science of Titanium Dioxide. *Surf. Sci. Rep.* **2003**, *48*, 53−229.

(12) Lukačević, I.; Gupta, S. K.; Jha, P. K.; Kirin, D. Lattice Dynamics and Raman Spectrum of Rutile TiO_2: The Role of Soft Phonon Modes in Pressure Induced Phase Transition. *Mater. Chem. Phys.* **2012**, *137*, 282−289.

(13) Reddy, B. M.; Khan, A.; Lakshmanan, P.; Aouine, M.; Loridant, S.; Volta, J.-C. Structural Characterization of Nanosized CeO_2-SiO_2, CeO_2-TiO_2, and CeO_2-ZrO_2 Catalysts By XRD, Raman, and HREM Techniques. *J. Phys. Chem. B* **2005**, *109*, 3355−3363.

(14) Hamze, N.; Dabir, B.; Kalbasi, M.; Derakhshan, A. A.; Rajabi, L.; Momeni, M. M. Synthesis and Characterization of MWCNT-Boehmite/TiO_2 Nanocomposite As an Excellent Oxidative Catalyst for Diesel Desulfurization. *J. Nanoeng. Nanomanuf.* **2012**, *2*, 234−240.

(15) Chiang, Y.-M.; Silverman, L. A.; French, R. H.; Cannon, R. M. Thin Glass Film Between Ultrafine Conductor Particles in Thick-Film Resistors. *J. Am. Ceram. Soc.* **1994**, *77*, 1143−1152.

(16) Lundin, U.; Fast, L.; Nordström, L.; Johansson, B.; Wills, J. M.; Eriksson, O. Transition-Metal Dioxides With a Bulk Modulus Comparable To Diamond. *Phys. Rev. B: Condens. Matter Mater. Phys.* **1998**, *57*, 4979−4982.

(17) Dubrovinsky, L. S.; Dubrovinskaia, N. A.; Swamy, V.; Muscat, J.; Harrison, N. M.; Ahuja, R.; Holm, B.; Johansson, B. Materials Science: The Hardest Known Oxide. *Nature* **2001**, *410*, 653−654.

(18) Hugosson, H. W.; Grechnev, G. E.; Ahuja, R.; Helmersson, U.; Sa, L.; Eriksson, O. Stabilization of Potential Superhard RuO_2 Phases: A Theoretical Study. *Phys. Rev. B: Condens. Matter Mater. Phys.* **2002**, *66*, 174111.

(19) Mattesini, M.; de Almeida, J. S.; Dubrovinsky, L.; Dubrovinskaia, N.; Johansson, B.; Ahuja, R. Cubic TiO_2 As a Potential Light Absorber in Solar-Energy Conversion. *Phys. Rev. B: Condens. Matter Mater. Phys.* **2004**, *70*, 115101.

(20) Kuo, M.-Y.; Chen, C.-L.; Hua, C.-Y.; Yang, H.-C.; Shen, P. Density Functional Theory Calculations of Dense TiO_2 Polymorphs: Implication for Visible-Light-Responsive Photocatalysts. *J. Phys. Chem. B* **2005**, *109*, 8693−8700.

(21) Olsen, J. S.; Gerward, L.; Jiang, J. On the rutile/α-PbO_2-type Phase Boundary of TiO_2. *J. Phys. Chem. Solids* **1999**, *60*, 229−233.

(22) Withers, A. C.; Essene, E. J.; Zhang, Y. Rutile/TiO_2-II Phase Equilibria. *Contrib. Mineral. Petrol.* **2003**, *145*, 199−204.

(23) Hashimoto, K.; Irie, H.; Fujishima, A. TiO_2 Photocatalysis: A Historical Overview and Future Prospects. *Jpn. J. Appl. Phys.* **2005**, *44*, 8269.

(24) Fang, J.; Bao, H.; He, B.; Wang, F.; Si, D.; Jiang, Z.; Pan, Z.; Wei, S.; Huang, W. Interfacial and Surface Structures of CeO_2-TiO_2 Mixed Oxides. *J. Phys. Chem. C* **2007**, *111*, 19078−19085.

(25) Wu, X.; Holbig, E.; Steinle-Neumann, G. Structural Stability of TiO_2 At High Pressure in Density-Functional Theory Based Calculations. *J. Phys.: Condens. Matter* **2010**, *22*, 295501.

(26) Tsai, M.-H.; Shen, P.; Chen, S.-Y. Defect Generation of Anatase Nanocondensates Via Coalescence and Transformation From Dense Fluorite-Type TiO_2. *J. Appl. Phys.* **2006**, *100*, 114313.

(27) Ataca, C.; Şahin, H.; Ciraci, S. Stable, Single-Layer MX_2 Transition-Metal Oxides and Dichalcogenides in a Honeycomb-Like Structure. *J. Phys. Chem. C* **2012**, *116*, 8983−8999.

(28) Haines, J.; Léger, J. M. Phase Transitions in Ruthenium Dioxide Up To 40 GPa: Mechanism for the Rutile-To-Fluorite Phase Transformation and a Model for the High-Pressure Behavior of Stishovite SiO_2. *Phys. Rev. B: Condens. Matter Mater. Phys.* **1993**, *48*, 13344−13350.

(29) Lagarec, K.; Desgreniers, S. Raman Study of Single Crystal Anatase TiO_2 Up To 70 GPa. *Solid State Commun.* **1995**, *94*, 519−524.

(30) Mattesini, M.; de Almeida, J. S.; Dubrovinsky, L.; Dubrovinskaia, N.; Johansson, B.; Ahuja, R. High-Pressure and High-Temperature Synthesis of the Cubic TiO_2 Polymorph. *Phys. Rev. B: Condens. Matter Mater. Phys.* **2004**, *70*, 212101.

(31) Swamy, V.; Wilson, N. C. First-Principles Calculations of the Pressure Stability and Elasticity of Dense TiO_2 Phases Using the B3LYP Hybrid Functional. *J. Phys. Chem. C* **2014**, *118*, 8617−8625.

(32) Mei, Z.-G.; Wang, Y.; Shang, S.; Liu, Z.-K. First-Principles Study of the Mechanical Properties and Phase Stability of TiO_2. *Comput. Mater. Sci.* **2014**, *83*, 114−119.

(33) Zhou, X.-F.; Dong, X.; Qian, G.-R.; Zhang, L.; Tian, Y.; Wang, H.-T. Unusual Compression Behavior of TiO_2 Polymorphs From First Principles. *Phys. Rev. B: Condens. Matter Mater. Phys.* **2010**, *82*, 060102.

(34) Pavasupree, S.; Ngamsinlapasathian, S.; Pivsa-art, S.; Suzuki, Y.; Yoshikawa, S. Synthesis, Characterization and Application of Single and Mixed Oxides Nanomaterials. *As. J. Energy Env.* **2005**, *6*, 193−201.

(35) Muñoz-Batista, M. J.; Gómez-Cerezo, M. N.; Kubacka, A.; Tudela, D.; Fernández-García, M. Role of Interface Contact in CeO_2-TiO_2 Photocatalytic Composite Materials. *ACS Catal.* **2014**, *4*, 63−72.

(36) Gorbenko, O. Y.; Samoilenkov, S. V.; Graboy, I. E.; Kaul, A. R. Epitaxial Stabilization of Oxides in Thin Films. *Chem. Mater.* **2002**, *14*, 4026−4043.

(37) Mehta, P.; Salvador, P. A.; Kitchin, J. R. Identifying Potential BO_2 Oxide Polymorphs for Epitaxial Growth Candidates. *ACS Appl. Mater. Interfaces* **2014**, *6*, 3630−3639.

(38) Chevrier, V. L.; Ong, S. P.; Armiento, R.; Chan, M. K. Y.; Ceder, G. Hybrid Density Functional Calculations of Redox Potentials and Formation Energies of Transition Metal Compounds. *Phys. Rev. B: Condens. Matter Mater. Phys.* **2010**, *82*, 075122.

DOI: 10.1021/acs.jpcc.5b05338
J. Phys. Chem. C 2015, 119, 21060−21071

(39) Akhade, S. A.; Kitchin, J. R. Effects of Strain, *d*-band Filling, and Oxidation State on the Surface Electronic Structure and Reactivity of 3*d* Perovskite Surfaces. *J. Chem. Phys.* **2012**, *137*, 084703.
(40) Jain, A.; Hautier, G.; Ong, S. P.; Moore, C. J.; Fischer, C. C.; Persson, K. A.; Ceder, G. Formation Enthalpies By Mixing GGA and GGA + *U* Calculations. *Phys. Rev. B: Condens. Matter Mater. Phys.* **2011**, *84*, 045115.
(41) Hautier, G.; Ong, S. P.; Jain, A.; Moore, C. J.; Ceder, G. Accuracy of Density Functional Theory in Predicting Formation Energies of Ternary Oxides From Binary Oxides and Its Implication on Phase Stability. *Phys. Rev. B: Condens. Matter Mater. Phys.* **2012**, *85*, 155208.
(42) Curnan, M. T.; Kitchin, J. R. Effects of Concentration, Crystal Structure, Magnetism, and Electronic Structure Method on First-Principles Oxygen Vacancy Formation Energy Trends in Perovskites. *J. Phys. Chem. C* **2014**, *118*, 28776−28790.
(43) Akhade, S. A.; Kitchin, J. R. Effects of Strain, *d*-band Filling, and Oxidation State on the Bulk Electronic Structure of Cubic 3*d* Perovskites. *J. Chem. Phys.* **2011**, *135*, 104702.
(44) Xu, Z.; Kitchin, J. R. Relating the Electronic Structure and Reactivity of the 3*d* Transition Metal Monoxide Surfaces. *Catal. Commun.* **2014**, *52*, 60−64.
(45) Ma, X. G.; Liang, P.; Miao, L.; Bie, S. W.; Zhang, C. K.; Xu, L.; Jiang, J. J. Pressure-Induced Phase Transition and Elastic Properties of TiO_2 Polymorphs. *Phys. Status Solidi B* **2009**, *246*, 2132−2139.
(46) Labat, F.; Baranek, P.; Domain, C.; Minot, C.; Adamo, C. Density Functional Theory Analysis of the Structural and Electronic Properties of TiO_2 Rutile and Anatase Polytypes: Performances of Different Exchange-correlation Functionals. *J. Chem. Phys.* **2007**, *126*, 154703.
(47) Koparde, V. N.; Cummings, P. T. Sintering of Titanium Dioxide Nanoparticles: a Comparison Between Molecular Dynamics and Phenomenological Modeling. *J. Nanopart. Res.* **2008**, *10*, 1169−1182.
(48) Barnard, A. S.; Zapol, P.; Curtiss, L. A. Modeling the Morphology and Phase Stability of TiO_2 Nanocrystals in Water. *J. Chem. Theory Comput.* **2005**, *1*, 107−116.
(49) Li, Q.; Liu, R.; Liu, B.; Wang, L.; Wang, K.; Li, D.; Zou, B.; Cui, T.; Liu, J.; Chen, Z.; et al. Stability and Phase Transition of Nanoporous Rutile TiO_2 Under High Pressure. *RSC Adv.* **2012**, *2*, 9052−9057.
(50) Swamy, V.; Dubrovinsky, L. S.; Dubrovinskaia, N. A.; Simionovici, A. S.; Drakopoulos, M.; Dmitriev, V.; Weber, H.-P. Compression Behavior of Nanocrystalline Anatase TiO_2. *Solid State Commun.* **2003**, *125*, 111−115.
(51) van Duin, A. C. T.; Dasgupta, S.; Lorant, F.; Goddard, W. A. Reaxff: A Reactive Force Field for Hydrocarbons. *J. Phys. Chem. A* **2001**, *105*, 9396−9409.
(52) Raju, M.; van Duin, A. C. T.; Fichthorn, K. A. Mechanisms of Oriented Attachment of TiO_2 Nanocrystals in Vacuum and Humid Environments: Reactive Molecular Dynamics. *Nano Lett.* **2014**, *14*, 1836−1842.
(53) Kim, S.-Y.; van Duin, A. C.; Kubicki, J. D. Molecular Dynamics Simulations of the Interactions Between TiO_2 Nanoparticles and Water With Na^+ and Cl^-, Methanol, and Formic Acid Using a Reactive Force Field. *J. Mater. Res.* **2013**, *28*, 513−520.
(54) Raju, M.; Kim, S.-Y.; van Duin, A. C. T.; Fichthorn, K. A. Reaxff Reactive Force Field Study of the Dissociation of Water on Titania Surfaces. *J. Phys. Chem. C* **2013**, *117*, 10558−10572.
(55) Kim, S.-Y.; van Duin, A. C. T. Simulation of Titanium Metal/titanium Dioxide Etching With Chlorine and Hydrogen Chloride Gases Using the Reaxff Reactive Force Field. *J. Phys. Chem. A* **2013**, *117*, 5655−5663.
(56) Kim, S.-Y.; Kumar, N.; Persson, P.; Sofo, J.; van Duin, A. C. T.; Kubicki, J. D. Development of a Reaxff Reactive Force Field for Titanium Dioxide/Water Systems. *Langmuir* **2013**, *29*, 7838−7846.
(57) Conesa, J. C. The Relevance of Dispersion Interactions for the Stability of Oxide Phases. *J. Phys. Chem. C* **2010**, *114*, 22718−22726.
(58) Wang, L.; Maxisch, T.; Ceder, G. Oxidation Energies of Transition Metal Oxides Within the GGA+U Framework. *Phys. Rev. B: Condens. Matter Mater. Phys.* **2006**, *73*, 195107.
(59) Liechtenstein, A. I.; Anisimov, V. I.; Zaanen, J. Density-Functional Theory and Strong Interactions: Orbital Ordering in Mott-Hubbard Insulators. *Phys. Rev. B: Condens. Matter Mater. Phys.* **1995**, *52*, R5467−R5470.
(60) Zhou, F.; Cococcioni, M.; Marianetti, C. A.; Morgan, D.; Ceder, G. First-Principles Prediction of Redox Potentials in Transition-Metal Compounds With LDA+U. *Phys. Rev. B: Condens. Matter Mater. Phys.* **2004**, *70*, 235121.
(61) Cohen, A. J.; Mori-Sánchez, P.; Yang, W. Insights Into Current Limitations of Density Functional Theory. *Science* **2008**, *321*, 792−794.
(62) Fahmi, A.; Minot, C.; Silvi, B.; Causá, M. Theoretical Analysis of the Structures of Titanium Dioxide Crystals. *Phys. Rev. B: Condens. Matter Mater. Phys.* **1993**, *47*, 11717−11724.
(63) Finazzi, E.; Di Valentin, C.; Pacchioni, G.; Selloni, A. Excess Electron States in Reduced Bulk Anatase TiO_2: Comparison of Standard GGA, GGA+U, and Hybrid DFT Calculations. *J. Chem. Phys.* **2008**, *129*, 154113.
(64) Morgan, B. J.; Watson, G. W. Intrinsic *n*-type Defect Formation in TiO_2: A Comparison of Rutile and Anatase From GGA+U Calculations. *J. Phys. Chem. C* **2010**, *114*, 2321−2328.
(65) Cococcioni, M.; de Gironcoli, S. Linear Response Approach To the Calculation of the Effective Interaction Parameters in the LDA+U Method. *Phys. Rev. B: Condens. Matter Mater. Phys.* **2005**, *71*, 035105.
(66) Mattioli, G.; Filippone, F.; Alippi, P.; Amore Bonapasta, A. Ab Initio Study of the Electronic States Induced By Oxygen Vacancies in Rutile and Anatase TiO_2. *Phys. Rev. B: Condens. Matter Mater. Phys.* **2008**, *78*, 241201.
(67) Mattioli, G.; Alippi, P.; Filippone, F.; Caminiti, R.; Amore Bonapasta, A. Deep Versus Shallow Behavior of Intrinsic Defects in Rutile and Anatase TiO_2 Polymorphs. *J. Phys. Chem. C* **2010**, *114*, 21694−21704.
(68) Swamy, V.; Dubrovinskaia, N. A.; Dubrovinsky, L. S. Compressibility of Baddeleyite-Type TiO_2 From Static Compression To 40 GPa. *J. Alloys Compd.* **2002**, *340*, 46−48.
(69) Ohsaka, T.; Yamaoka, S.; Shimomura, O. Effect of Hydrostatic Pressure on the Raman Spectrum of Anatase (TiO_2). *Solid State Commun.* **1979**, *30*, 345−347.
(70) Mammone, J.; Sharma, S.; Nicol, M. Raman Study of Rutile (TiO_2) At High Pressures. *Solid State Commun.* **1980**, *34*, 799−802.
(71) Arashi, H. Raman Spectroscopic Study of the Pressure-Induced Phase Transition in TiO_2. *J. Phys. Chem. Solids* **1992**, *53*, 355−359.
(72) Sekiya, T.; Ohta, S.; Kamei, S.; Hanakawa, M.; Kurita, S. Raman Spectroscopy and Phase Transition of Anatase TiO_2 Under High Pressure. *J. Phys. Chem. Solids* **2001**, *62*, 717−721.
(73) Arlt, T.; Bermejo, M.; Blanco, M. A.; Gerward, L.; Jiang, J. Z.; Staun Olsen, J.; Recio, J. M. High-Pressure Polymorphs of Anatase TiO_2. *Phys. Rev. B: Condens. Matter Mater. Phys.* **2000**, *61*, 14414−14419.
(74) Arroyo-de Dompablo, M. E.; Morales-García, A.; Taravillo, M. DFT+U Calculations of Crystal Lattice, Electronic Structure, and Phase Stability Under Pressure of TiO_2 Polymorphs. *J. Chem. Phys.* **2011**, *135*, 054503.
(75) Kulik, H. J.; Cococcioni, M.; Scherlis, D. A.; Marzari, N. Density Functional Theory in Transition-Metal Chemistry: A Self-Consistent Hubbard *U* Approach. *Phys. Rev. Lett.* **2006**, *97*, 103001.
(76) Muscat, J.; Swamy, V.; Harrison, N. M. First-Principles Calculations of the Phase Stability of TiO_2. *Phys. Rev. B: Condens. Matter Mater. Phys.* **2002**, *65*, 224112.
(77) Murnaghan, F. The Compressibility of Media Under Extreme Pressures. *Proc. Natl. Acad. Sci. U. S. A.* **1944**, *30*, 244.
(78) Kresse, G.; Furthmüller, J. Efficient Iterative Schemes for Ab Initio Total-Energy Calculations Using a Plane-Wave Basis Set. *Phys. Rev. B: Condens. Matter Mater. Phys.* **1996**, *54*, 11169−11186.
(79) Hammouchi, M.; El Boudouti, E. H.; Nougaoui, A.; Djafari-Rouhani, B.; Lahlaouti, M. L. H.; Akjouj, A.; Dobrzynski, L. Acoustic

DOI: 10.1021/acs.jpcc.5b05338
J. Phys. Chem. C 2015, 119, 21060−21071

Waves in Finite Superlattices: Influence of Buffer Layers. *Phys. Rev. B: Condens. Matter Mater. Phys.* **1999**, *59*, 1999−2010.
(80) Blöchl, P. E. Projector Augmented-Wave Method. *Phys. Rev. B: Condens. Matter Mater. Phys.* **1994**, *50*, 17953−17979.
(81) Perdew, J. P.; Zunger, A. Self-Interaction Correction To Density-Functional Approximations for Many-Electron Systems. *Phys. Rev. B: Condens. Matter Mater. Phys.* **1981**, *23*, 5048−5079.
(82) Perdew, J. P.; Burke, K.; Ernzerhof, M. Generalized Gradient Approximation Made Simple. *Phys. Rev. Lett.* **1996**, *77*, 3865−3868.
(83) Perdew, J. P.; Ruzsinszky, A.; Csonka, G. I.; Vydrov, O. A.; Scuseria, G. E.; Constantin, L. A.; Zhou, X.; Burke, K. Restoring the Density-Gradient Expansion for Exchange in Solids and Surfaces. *Phys. Rev. Lett.* **2008**, *100*, 136406.
(84) Armiento, R.; Mattsson, A. E. Functional Designed To Include Surface Effects in Self-Consistent Density Functional Theory. *Phys. Rev. B: Condens. Matter Mater. Phys.* **2005**, *72*, 085108.
(85) Perdew, J. P.; Chevary, J. A.; Vosko, S. H.; Jackson, K. A.; Pederson, M. R.; Singh, D. J.; Fiolhais, C. Atoms, Molecules, Solids, and Surfaces: Applications of the Generalized Gradient Approximation for Exchange and Correlation. *Phys. Rev. B: Condens. Matter Mater. Phys.* **1992**, *46*, 6671−6687.
(86) Dudarev, S.; Botton, G.; Savrasov, S.; Humphreys, C.; Sutton, A. Electron-Energy-Loss Spectra and the Structural Stability of Nickel Oxide: An LSDA + *U* Study. *Phys. Rev. B: Condens. Matter Mater. Phys.* **1998**, *57*, 1505−1509.
(87) Monkhorst, H. J.; Pack, J. D. Special Points for Brillouin-Zone Integrations. *Phys. Rev. B* **1976**, *13*, 5188−5192.
(88) Perdew, J. P.; Ernzerhof, M.; Burke, K. Rationale for Mixing Exact Exchange With Density Functional Approximations. *J. Chem. Phys.* **1996**, *105*, 9982−9985.
(89) Heyd, J.; Scuseria, G. E.; Ernzerhof, M. Hybrid Functionals Based on a Screened Coulomb Potential. *J. Chem. Phys.* **2003**, *118*, 8207−8215.
(90) Heyd, J.; Scuseria, G. E.; Ernzerhof, M. Erratum: Hybrid functionals based on a screened Coulomb potential [J. Chem. Phys.118, 8207 (2003)]. *J. Chem. Phys.* **2006**, *124*, 219906−1.
(91) Cococcioni, M.; de Gironcoli, S. A LDA + *U* Study of Selected Iron Compounds. Ph.D. Thesis, 2002.
(92) Tsuneda, T.; Hirao, K. Self-Interaction Corrections in Density Functional Theory. *J. Chem. Phys.* **2014**, *140*, 18A513.
(93) Kulik, H. J.; Marzari, N. Systematic Study of First-Row Transition-Metal Diatomic Molecules: A Self-Consistent DFT+*U* Approach. *J. Chem. Phys.* **2010**, *133*, 114103.
(94) Hu, Z.; Metiu, H. Choice of U for DFT+U Calculations for Titanium Oxides. *J. Phys. Chem. C* **2011**, *115*, 5841−5845.
(95) De Angelis, F.; Di Valentin, C.; Fantacci, S.; Vittadini, A.; Selloni, A. Theoretical Studies on Anatase and Less Common TiO_2 Phases: Bulk, Surfaces, and Nanomaterials. *Chem. Rev.* **2014**, *114*, 9708−9753. PMID: 24926899
(96) Agapito, L. A.; Curtarolo, S.; Buongiorno Nardelli, M. Reformulation of DFT+*U* As a Pseudohybrid Hubbard Density Functional for Accelerated Materials Discovery. *Phys. Rev. X* **2015**, *5*, 011006.
(97) Han, X.; Shao, G. Electronic Properties of Rutile TiO_2 With Nonmetal Dopants From First Principles. *J. Phys. Chem. C* **2011**, *115*, 8274−8282.
(98) Islam, M. M.; Calatayud, M.; Pacchioni, G. Hydrogen Adsorption and Diffusion on the Anatase TiO_2(101) Surface: A First-Principles Investigation. *J. Phys. Chem. C* **2011**, *115*, 6809−6814.
(99) Han, X.; Song, K.; Lu, L.; Deng, Q.; Xia, X.; Shao, G. Limitation and Extrapolation Correction of the Gga+ U Formalism: a Case Study of Nb-Doped Anatase TiO_2. *J. Mater. Chem. C* **2013**, *1*, 3736−3746.
(100) Xu, Z.; Rossmeisl, J.; Kitchin, J. R. A Linear Response DFT+U Study of Trends in the Oxygen Evolution Activity of Transition Metal Rutile Dioxides. *J. Phys. Chem. C* **2015**, *119*, 4827−4833.
(101) Giannozzi, P.; Baroni, S.; Bonini, N.; Calandra, M.; Car, R.; Cavazzoni, C.; Ceresoli, D.; Chiarotti, G. L.; Cococcioni, M.; Dabo, I.; et al. Quantum Espresso: a Modular and Open-Source Software Project for Quantum Simulations of Materials. *J. Phys.: Condens. Matter* **2009**, *21*, 395502.
(102) Garrity, K. F.; Bennett, J. W.; Rabe, K. M.; Vanderbilt, D. Pseudopotentials for High-Throughput DFT Calculations. *Comput. Mater. Sci.* **2014**, *81*, 446−452.
(103) Kulik, H. J.; Marzari, N. A Self-Consistent Hubbard *U* Density-Functional Theory Approach To the Addition-Elimination Reactions of Hydrocarbons on Bare FeO^+. *J. Chem. Phys.* **2008**, *129*, 134314.
(104) Kulik, H. J.; Marzari, N. Accurate Potential Energy Surfaces With a DFT+$U(R)$ Approach. *J. Chem. Phys.* **2011**, *135*, 194105.
(105) Gerosa, M.; Bottani, C. E.; Caramella, L.; Onida, G.; Di Valentin, C.; Pacchioni, G. Electronic Structure and Phase Stability of Oxide Semiconductors: Performance of Dielectric-Dependent Hybrid Functional DFT, Benchmarked Against *GW* Band Structure Calculations and Experiments. *Phys. Rev. B: Condens. Matter Mater. Phys.* **2015**, *91*, 155201.
(106) Rao, C. N. R. Kinetics and Thermodynamics of the Crystal Structure Transformation of Spectroscopically Pure Anatase To Rutile. *Can. J. Chem.* **1961**, *39*, 498−500.
(107) Kitchin, J. R.; Reuter, K.; Scheffler, M. Alloy Surface Segregation in Reactive Environments: First-Principles Atomistic Thermodynamics Study of Ag_3Pd(111) in Oxygen Atmospheres. *Phys. Rev. B: Condens. Matter Mater. Phys.* **2008**, *77*, 075437.
(108) Smith, S. J.; Stevens, R.; Liu, S.; Li, G.; Navrotsky, A.; Boerio-Goates, J.; Woodfield, B. F. Heat Capacities and Thermodynamic Functions of TiO_2 Anatase and Rutile: Analysis of Phase Stability. *Am. Mineral.* **2009**, *94*, 236−243.
(109) Shirley, R.; Kraft, M.; Inderwildi, O. R. Electronic and Optical Properties of Aluminium-doped Anatase and Rutile TiO_2 from *Ab Initio* Calculations. *Phys. Rev. B: Condens. Matter Mater. Phys.* **2010**, *81*, 075111.
(110) Moellmann, J.; Ehrlich, S.; Tonner, R.; Grimme, S. A DFT-D Study of Structural and Energetic Properties of TiO_2 Modifications. *J. Phys.: Condens. Matter* **2012**, *24*, 424206.
(111) Alkauskas, A.; Broqvist, P.; Pasquarello, A. Defect Levels Through Hybrid Density Functionals: Insights and Applications. *Phys. Status Solidi B* **2011**, *248*, 775−789.

DOI: 10.1021/acs.jpcc.5b05338
J. Phys. Chem. C 2015, 119, 21060−21071